Monte–Carlo simulation of the collapse transition of a two-dimensional polymer

T. M. Birshtein, S. V. Buldyrev and A. M. Elyashevitch
Institute of Macromolecular Compounds of the Academy of Sciences of the USSR, Leningrad, USSR
(Received 18 February 1985)

Two-dimensional self-avoiding lattice chains with the attraction of monomers are studied by the Monte–Carlo method. A new version of the simulation technique is described. The dependence of the chain sizes, number of contacts and specific heat on the temperature and number of links are obtained and the existence of the collapse transition is proved. The precise determination of the θ-point, tricritical exponent ν_t and crossover exponent ϕ based on the scaling treatment yielded: $\theta = 1.54$, $\nu_t = 0.59$, $\phi = 0.6$. This is in good agreement with recent theoretical predictions and experimental data. The relation with early works is also discussed.

Keywords: polymer solution; collapse transition; two-dimensional lattice model; Monte-Carlo method; scaling; theta-point; tricritical exponents

INTRODUCTION

The practical and theoretical studies of isolated polymer chain conformations in two dimensions are interesting when related to the investigations of polymer monolayers, and adsorption phenomenona etc.

A great number of theoretical works[1-11] have been devoted to the problem of the collapse of molecular coils in two dimensions. However, there is some discrepancy between the results of different authors.

The existence of the critical θ-temperature in two dimensions ($d=2$) as well as in three dimensions ($d=3$) is generally now acknowledged. Above the θ-point molecular coils swell, and the mean-square of end-to-end distance R^2 becomes proportional to $N^{3/2}$ (N is the number of links). Below the θ-point coils collapse into dense globules in which $R^2 \sim N$. This result follows[12] from the mean-field theory[13]. In three-dimensional space $R^2 \sim N^{6/5}$ for $T>\theta$, $R^2 \sim N^{2/3}$ for $T<\theta$, and $R^2 \sim N$ at the θ-point, i.e. chains behave as random coils and the excluded volume effects are practically compensated by the attractive forces between monomers, if one neglects the logarithmic corrections. The behaviour of chains at the θ-point in two dimensional case, character of temperature dependence of the sizes of globular and coil chains are still in the focus of discussion and require further investigation.

There are several results of numerical experiments in the literature, obtained by different modifications of the Monte-Carlo method. These data are in good agreement with each other, but their interpretation is rather ambiguous, and depends on the theoretical concepts of the authors.

In the present work we carry out the numerical simulation of two-dimensional chains on the square lattice taking into account the attraction of monomers. The model and Monte-Carlo technique are fully described later. The aim of our work is to study the behaviour of two-dimensional chains in different conditions and to determine the critical exponents. We pay particular attention to the adequate analysis of the numerical experiment and we show later that the correct determination of the θ-point is a problem.

MODEL

We use the well known Rosenbluthes version of the Monte-Carlo method[17]. A conformation of the macromolecule consisting of $N+1$ monomers is represented by a random self-avoiding walk of N steps on the two-dimensional square lattice. The attraction of monomers is introduced, as it has been done in Refs 18–20. In order to increase the probability of the appearence of high-number-of-contacts conformations which make the major contribution to the partition function in the case of nonzero attractive energy, we use the following method. Assuming that the end of the walk, j-1 steps long, is in the lattice site (X, Y), let each of the neighbouring sites vacant for the jth step have a number $K_j = 1,2,\ldots,\sigma_j$, where $\sigma_j \leqslant 3$ is a total number of these sites. Each of these σ_j sites is, in turn, in contact with $0 \leqslant \eta_{k_j} \leqslant 3$ occupied sites. Giving priority to the sites with greater values of η_{k_j}, we shall pass to site K_j with probability:

$$P_{k_j} = \frac{\rho_{k_j}}{\sum_{i_j=1}^{\sigma_j} \rho_{i_j}}, \qquad \rho_{k_j} = e^{\psi \eta_{k_j}} \tag{1}$$

where ψ is some positive constant which we name the construction potential (com. 21). The ensembles with various ψ have been constructed. The method of calculation of different average values, taking into account the value of ψ, and method of selection of the optimum value of ψ are described later.

σ_j may, sometimes, be zero. In this case, the chain should be rejected, and should be included only in the ensembles of chains consisting of $N \leqslant j-1$ links. In the two dimensional model such a marked procedure leads to the elimination of chains.

The situation may be improved if we examine two steps ahead and forbid walks leading to the sites for which

0032-3861/85/121814-11$03.00

$\eta_{k_j}=3$ (i.e. let $\rho_{k_j}=0$), since such walks will immediately lead to the death of the chain on the following step. But large elimination of chains is still preserved. The data, obtained for $\psi=0.3$, show that the probability for the 19 links chains to grow up to 199 links is approximately 0.16. The probability of passing the next twenty steps gradually diminishes from 0.9 for $N=19$ to 0.8 for $N=179$.

These difficulties can be ignored if we use ensembles of a special type of walks which we shall name infinitely-prolonging walks (IPW's), defined as follows: the end of such a walk cannot locate itself in a region boarded by previous links of the chain, so that there is no path leading out of this region for a self-avoiding walk. The N-long IPW's represent a rather poor subset of the whole set of all arbitrary self-avoiding walks (SAW's) of the same length. Apparently, the ratio of the number of all IPW's of the length N to the number of all SAW's of the same length tends to zero when N tends to infinity. Therefore the mean-square of end-to-end distance R^2, the mean square of radius of gyration S^2, the mean energy per monomer U, calculated for SAW and IPW ensembles, may be different. We dwell, mainly, upon the study of IPW ensembles. The comparison with the data for the ensemble of 80000 SAW's (see *Table 1*) in the interval of temperatures close to the θ-point, is given in *Table 4*, see also *Figures 6*, *7* and *Table 6*.

The algorithm for construction of an IPW is based on computation of the angle α_j between the vector of the last jth step and the vector of the first. If the jth link collides with the kth one, the value $\alpha_j-\alpha_k$ is to be examined, and if it is positive the non-normalized probability of the left turn $\rho_{l_{j+1}}$ (see equation (1)) should be equal to 0. On the contrary, if $\alpha_j-\alpha_k<0$, the right turn should be forbidden. It is obvious, that $\alpha_j-\alpha_k$ cannot be equal to zero. Inspite of the fact that the computer program realizing such an algorithm is rather complicated, it turns out to be twice as effective as the ordinary program generating all SAW's. At larger N its relative efficiency is even higher, because the computation time in the case of IPW's depends on N linearly (all the chains grow up to the given value of N), while in the case of SAW's—exponentialy, as their probability to grow up to the given value is proportional to $e^{-\lambda N}$.

METHOD OF ENSEMBLE AVERAGING

In order to evaluate a correct ensemble average the weight factor $w_q=1/(3^{N-2}P_q)$ should be used[17], where P_q is the probability of a given qth walk:

$$P_q=\prod_{j=1}^{N}P_{k_{jq}}=\prod_{j=1}^{N}\frac{e^{\psi\eta k_{jq}}}{\sum_{i_{jq}=1}^{\sigma_{jq}}e^{\psi\eta i_{jq}}} \tag{2}$$

In this formula $K_{jq}=1, 2, \sigma_{jq}$ are the numbers of sites which were chosen on the jth step of the qth walk. The numerical factor 3^{-N+2} prevents too large values of W_q. The ensemble average is calculated according to the formula:

$$\langle v\rangle=\frac{\sum_{q=1}^{M}v_q f_q}{\sum_{q=1}^{M}f_q},\qquad f_q=w_q\,e^{\phi\eta_q} \tag{3}$$

where v_q is the value of the averaging quantity for qth chain of the ensemble, M is the total number of chains in the ensemble, f_q is the partition function of qth walk, w_q is the Rosenbluthes factor of qth chain, $\Phi=-\varepsilon/kT$ is the energy of attraction between monomers situated in the nearest-neighbour lattice sites, $\eta_q=\sum_{j=1}^{N}\eta_{k_{jq}}$ is the total number of contacts in the qth walk.

We determined the mean-square radius of gyration $\langle S^2\rangle$, the mean square end-to-end distance $\langle R^2\rangle$, the mean energy per monomer $\langle U\rangle=\langle\eta\rangle\phi/(N+1)$, the mean specific heat per monomer $\langle C\rangle=\Phi^2/(N+1)(\langle\eta^2\rangle-\langle\eta\rangle^2)$. (Wherever it is possible, the '$\langle\rangle$' brackets of mean values will be omitted. E.g. we will write R^2 instead of $\langle R^2\rangle$.)

The data were obtained for several ensembles of 60000–140000 chains $N=199$ links long with different construction potentials ψ. For each ensemble, the averaging was carried out for 5 different interaction energies ϕ (see *Table 1*). All the quantities were being averaged in the process of generating of chains, as they became 19, 39, ..., 199 links long. Thus, for each ensemble of 199-link chains, 9 ensembles of shorter chains were obtained, each being the initial part of a coresponding chain of 199 links. These ensembles of different lengths N cannot be considered as statistically independent. However, the character of the dependence of the chain properties on N can be observed more easily for such a set of ensembles. The variance of averages is computed over 4–10 sub-ensembles consisting of 10000–20000 chains. The spread of values of the averages computed in different ensembles do not exceed the bounds of the confidence interval evaluated by sub-ensembles of a single ensemble.

Table 1 List of ensembles over which the averaging was carried out. Ensembles I–IV consist of IPW's, ensemble VII consists of SAW's; the maximal chain length in each ensemble is 199

No.	Ψ	$M/10^3$	Φ
I	0.0	80	0.2–(0.1)–0.6
II	0.1	60	0.2–(0.1)–0.6
III	0.25	75	0.60–(0.05)–0.80
IV	0.3	60	0.60–(0.025)–0.70
V	0.4	140	0.70–(0.05)–0.90
VI	0.6	60	0.70–(0.05)–0.90
VII	0.3	80	0.60–(0.025)–0.675

Ψ-construction potential
M-total number of chains in the ensemble
Φ-attractive energy of monomers

OPTIMUM VALUE OF THE CONSTRUCTION POTENTIAL

The mathematical probability of any ensemble average as well as the probability of partition function f_q is independent of the value of ψ:

$$E(f_q)=\sum_q P_q f_q=\sum_q P_q w_q\,e^{\phi\eta_q}=3^{2-N}\sum_q e^{\phi\eta_q}$$

where the sum is taken over all chains of the length N. But the variance $V(f_q)$ depends on ψ and can be sufficiently decreased by its choice:

$$V(f_q)=3^{2-N}\sum_q w_q\,e^{-2\phi\eta_q}-E^2(f_q)$$

Instead of calculating the variance we calculated the effective number of chains:

$$M_{\text{eff}}=\sum_{q=1}^{M}f_q/\max_q\{f_q\}$$

yielding a sufficient contribution to the partition function. M_{eff} also depends on ψ. As it follows from the examination

of short chains with 4 links, it can be asserted that in order to attain the highest M_{eff}, one should take $\psi \leqslant \Phi$. It is easy to show that the optimum value of construction potential in the case of sufficiently large M is given by:

$$\psi_{opt}(\Phi)|_{N=4} = \begin{cases} \Phi, & \Phi < \ln 2 \approx 0.69 \\ \ln 2, & \Phi \geqslant \ln 2 \end{cases}$$

The dependence of M_{eff} on Φ for different ψ values for the ensembles of 60 000 19- and 199-links chains is shown in *Figure 1a*. The families of curves, corresponding to different values of ψ, have the envelopes with maximum at $\Phi = 0.5$–0.65, which drifts to the right with the increase of N. The existence of a bell-form envelope suggests that the introduction of the construction potential ψ is most effective near the θ-point, $\Phi_\theta \approx 0.65$. This result has something in common with Ref. 18, where the highest accuracy has also been marked in the vicinity of θ-point. The value of $\psi_{opt}(\Phi)$ is shown in *Figure 1b*.

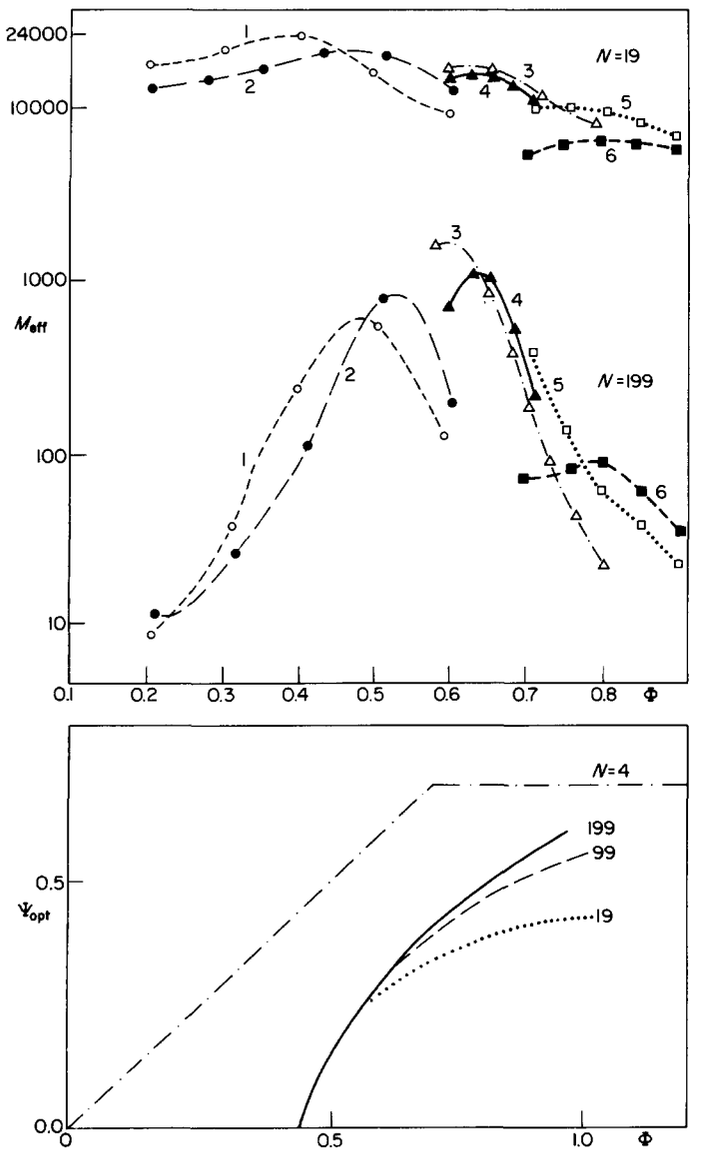

Figure 1 (a) The effective number of chains M_{eff} vs. Φ for the ensembles of 60 000 chains of $N = 19$ and 199 links, generated with different values of the construction potential Ψ. The values of Ψ for curves 1–6 are $\Psi = 0.00$, $\Psi = 0.10$, $\Psi = 0.25$, $\Psi = 0.30$, $\Psi = 0.4$ and $\Psi = 0.60$; (b) The influence of the attractive energy Φ on the optimum value of construction potential Ψ_{opt} for different chain lengthes N. The curve for $N = 4$ have been obtained theoretically

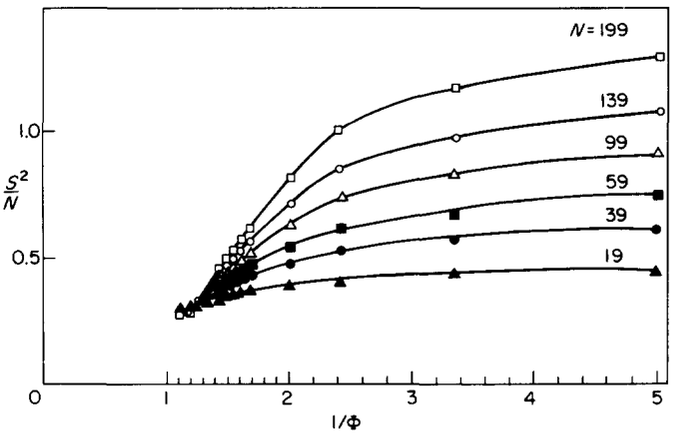

Figure 2 S^2/N vs. $1/\Phi = -kT/\varepsilon$ for various values of N (figures on the curves), obtained for IPW's on the grounds of our numerical experiment

DEPENDENCE OF THE CHAIN SIZES ON N AND τ

The results of the numerical computation of the chain-size dependence on the temperature $1/\Phi = -kT/\varepsilon$ are given in *Figure 2*. A number of parameters are determined from these results: (1) the location of the θ-point; (2) exponent ν_t specifying the molecular-mass dependence of the size at the θ-point $S_\theta^2 \sim N^{2\nu_t}$; (3) the exponents specifying the molecular-mass and temperature dependences in the extended coil in the good solvent (index +), and in the globular state (index −). It should be emphasized that the situation is more complicated than in the 3-dimensional case, where the random-coil behaviour of chains at the θ-point is already known. In the two-dimensional case one should also proceed with the appropriate theoretical premises.

The most general expression for the chain sizes is yielded by the scaling theory[1], according to which:

$$S^2 \sim N^{2\nu_t} f(N^\phi \tau) \tag{4}$$

where ν_t is the tricritical exponent specifying the chain sizes in the critical θ-region, φ is the cross-over exponent, $\tau = (T-\theta)/\theta$ is the reduced temperature and $f(x)$ is a function having the following asymptotics:

$$f(x) = \begin{cases} x^{\mu_+}, & x \to +\infty \\ |x|^{-\mu_-}, & x \to -\infty \end{cases} \tag{5}$$

and turning into 1 for $x = 0$.

The exponents μ_+ and μ_- are related to ν_t, and ϕ by

$$\mu_+ = \frac{\frac{3}{2} - 2\nu_t}{\phi}$$

$$\mu_- = \frac{2\nu_t - 1}{\phi} \tag{6}$$

which ensure the well known conditions[6–9]:

$$S_+^2 \sim N^{3/2}, \quad S_-^2 \sim N$$

As to the numerical values of exponents ν_t, φ, μ_+, μ_-, the theoretical data available in literature are contradictory. These data are sumarized in *Table 2*. (It is to be noted that the formulae of *Table 2* give the main terms of asymptotics for $N \to \infty$ and $\tau \ll 1$, the proportionality factors being omitted).

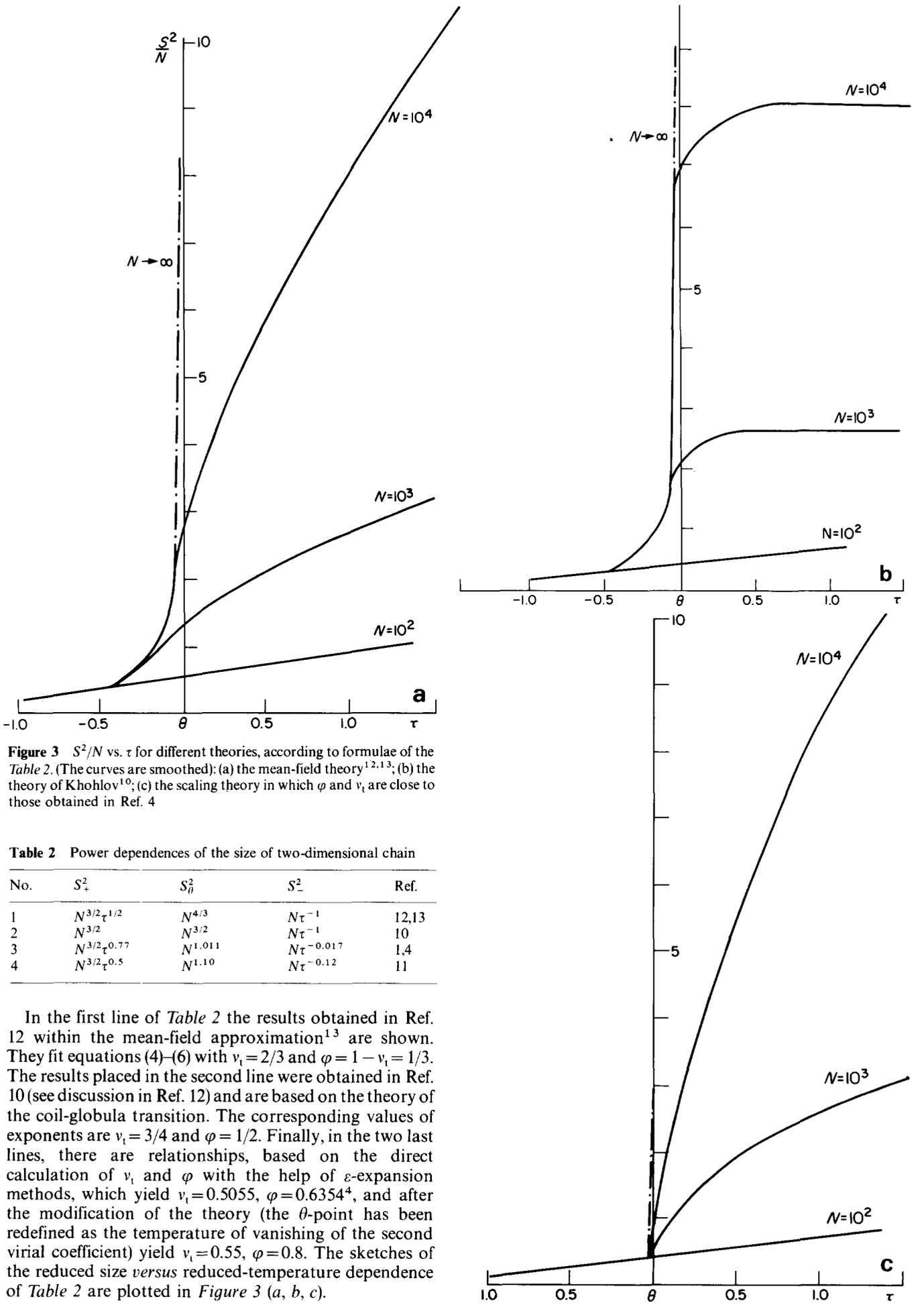

Figure 3 S^2/N vs. τ for different theories, according to formulae of the *Table 2*. (The curves are smoothed): (a) the mean-field theory[12,13]; (b) the theory of Khohlov[10]; (c) the scaling theory in which φ and ν_t are close to those obtained in Ref. 4

Table 2 Power dependences of the size of two-dimensional chain

No.	S_+^2	S_θ^2	S_-^2	Ref.
1	$N^{3/2}\tau^{1/2}$	$N^{4/3}$	$N\tau^{-1}$	12,13
2	$N^{3/2}$	$N^{3/2}$	$N\tau^{-1}$	10
3	$N^{3/2}\tau^{0.77}$	$N^{1.011}$	$N\tau^{-0.017}$	1,4
4	$N^{3/2}\tau^{0.5}$	$N^{1.10}$	$N\tau^{-0.12}$	11

In the first line of *Table 2* the results obtained in Ref. 12 within the mean-field approximation[13] are shown. They fit equations (4)–(6) with $\nu_t = 2/3$ and $\varphi = 1 - \nu_t = 1/3$. The results placed in the second line were obtained in Ref. 10 (see discussion in Ref. 12) and are based on the theory of the coil-globula transition. The corresponding values of exponents are $\nu_t = 3/4$ and $\varphi = 1/2$. Finally, in the two last lines, there are relationships, based on the direct calculation of ν_t and φ with the help of ε-expansion methods, which yield $\nu_t = 0.5055$, $\varphi = 0.6354$[4], and after the modification of the theory (the θ-point has been redefined as the temperature of vanishing of the second virial coefficient) yield $\nu_t = 0.55$, $\varphi = 0.8$. The sketches of the reduced size *versus* reduced-temperature dependence of *Table 2* are plotted in *Figure 3* (*a*, *b*, *c*).

The visual comparison of these curves with each other and with the experimental data of *Figure 2* shows that the data can be made to agree with each plot of *Figure 3* (*a,b,c*), by varying the location of the θ-point. In this way, we start the analysis of our data by determination of the θ-point, using equation (4) as an ansatz.

DETERMINATION OF THE θ-POINT AND THE EXPONENT ν_t

Figure 4 illustrates the molecular-mass dependence of the reduced chain sizes S^2 and R^2. The computation errors are given in *Table 3*. The comparison of the data for IPW's and SAW's is given in *Table 4*. The straight lines of *Figure 4* correspond to the ideal random-walk chains without immediate reversals on the square lattice. The well known formulae of conformational statistics[23,24] for such chains give:

$$S^2/N = 1/3 - 5/(12N) + 0(1/N^2)$$
$$R^2/N = 2 - 3(1 - 1/3^N)/(2N) \quad (7)$$

For two-dimensional chains, the value of S^2/N is inversely-proportional to the chain density which appears to be finite for random chains even when $N \to \infty$. The limiting value of density for a completely compact globular chain is $S^2/N = 1/(2\pi)$ when $N \to \infty$. As can be seen from *Figure 4*, the chain sizes at high energies Φ ($\Phi \geqslant 0.75$–0.8) appear to be not larger than those of random-coil. The chain sizes per link diminish with the increasing N, i.e. the density increase with chain length. (In several cases the sizes per link pass through the maximum with

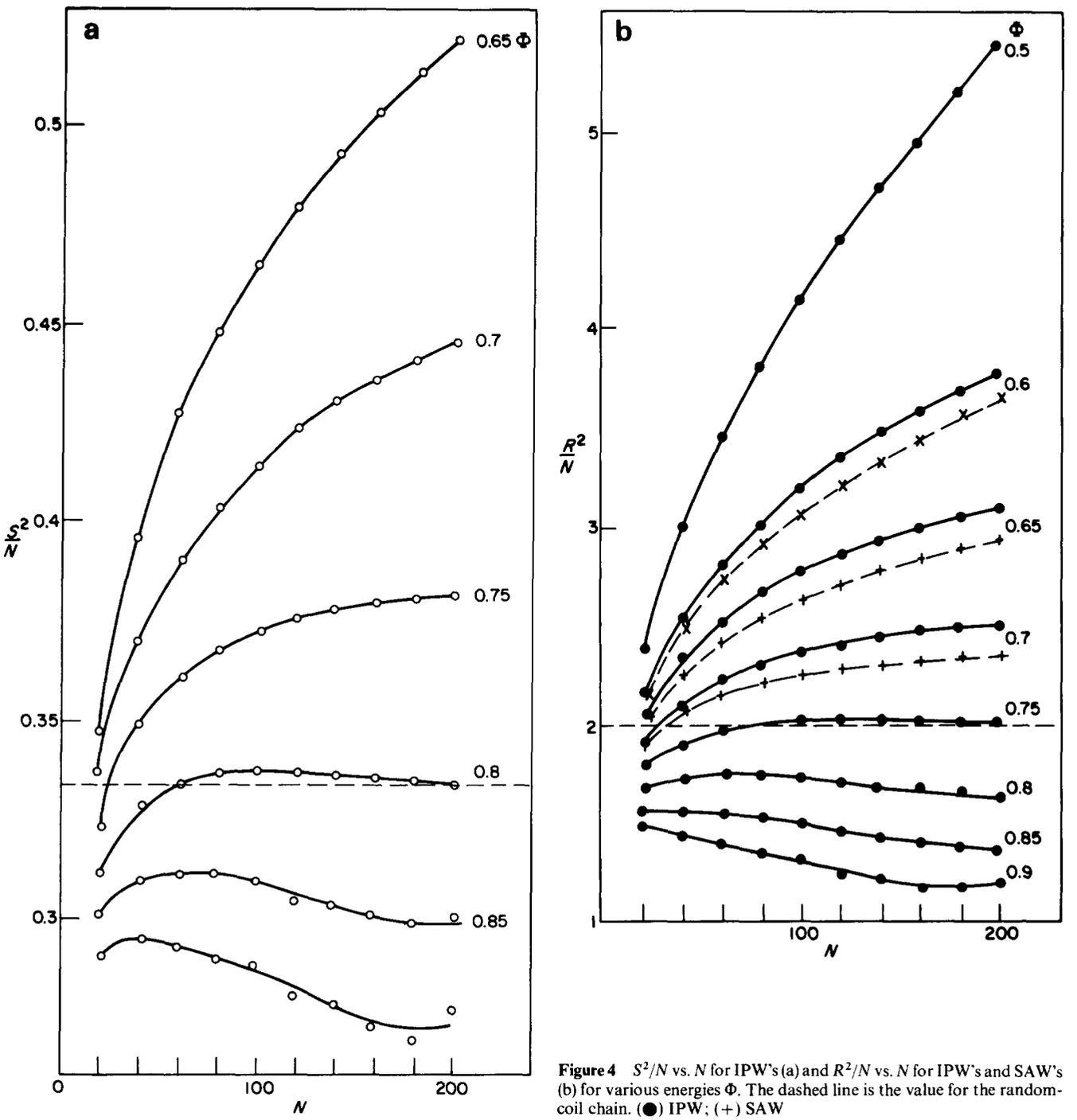

Figure 4 S^2/N vs. N for IPW's (a) and R^2/N vs. N for IPW's and SAW's (b) for various energies Φ. The dashed line is the value for the random-coil chain. (●) IPW; (+) SAW

increasing N). Obviously this situation corresponds to the conditions below the θ-point ($\Phi > \Phi_0$).

For more detailed study, we plotted the log–log molecular-mass dependence of chain sizes (see *Figure 5*). The slopes of these curves calculated according to the formulae $\ln X^2 = \gamma_X \ln N + B_X$, where $X = S$; R, are shown in *Figures 6*, *7* and in *Table 5*. The linear representations of the dependences in question were calculated by the least-square method for groups of several neighbour points, the values of the slopes γ_X and terms B_X being assigned to the point $\bar{N}$ which is the geometric mean of chain lengths for each group.

The data of *Figures 6* and *7* and *Table 5* were obtained for groups of three and five points. The analysis of the curves in *Figure 5* has also been carried out, using more the general representation $\ln X^2 = \gamma_X \ln(N+\kappa) + B_X$. The introduction of the correction term κ, suggested by the structure of equation (7), does not practically influence the main conclusions. For $\kappa = \pm 1$, the dependence of γ_x vs. N within the interval of $\phi = 0.6$–0.7 becomes non-monotone. The root-mean-square errors of the determined values of γ_s are given in *Table 5*. They are obtained by calculating

Table 3 The mean square radius of gyration $\langle S^2 \rangle$, its coefficient of variation

$$\delta(S^2) = \left(\sum_{i=1}^{M/M_1} (\langle S^2 \rangle_i - \langle S^2 \rangle)^2 \right)^{1/2} \Big/ \left(\sqrt{\frac{M}{M_1}\left(\frac{M}{M_1} - 1\right)} \langle S^2 \rangle \right)$$

and effective number of chains M_{eff} in various ensembles. The length of each chain is $N = 199$ links, M-total number of chains in the ensembles, M_1-the number of chains in the subensembles that were used for calculation of σ. The averaging over ith subensemble is marked by index i below the angle brackets

	Ensemble I			Ensemble III			Ensemble V		
	$\Psi = 0.0$, $M = 80\,000$, $M_1 = 20\,000$			$\Psi = 0.25$, $M = 75\,000$, $M_1 = 15\,000$			$\Psi = 0.4$, $M = 140\,000$ $M_1 = 10\,000$		
ϕ	S^2	$\sigma(S^2)$	M_{eff}	S^2	$\sigma(S^2)$	M_{eff}	S^2	$\sigma(S^2)$	M_{eff}
0.2	263	5%	14						
0.3	233	2%	43						
0.4	200.3	1%	274						
0.5	162.2	0.3%	614						
0.6	120.8	0.8%	99	122.0	0.3%	1858			
0.7				88.0	0.4%	282	88.7	0.2%	691
0.8				66.2	1.4%	29	66.7	0.4%	101
0.9							55.2	1.4%	12

Table 4 Comparison of R^2, S^2, U for IPW- and SAW-ensembles (ensembles IV and VII of *Table 1*, $\Psi = 0.3$). The last nonzero digit in the values of R^2, S^2, U is a significant one

		R^2			S^2			U		
N	Φ	0.6	0.65	0.7	0.6	0.65	0.7	0.6	0.65	0.7
19	IPW	40.6	38.3	36.1	6.80	6.56	6.33	0.172	0.197	0.222
	SAW	40.3	38.0	35.8	6.76	6.52	6.29	0.174	0.197	0.222
99	IPW	310	290	230	51	46	41	0.245	0.286	0.332
	SAW	300	260	220	50	45	40	0.247	0.289	0.333
199	IPW	760	620	500	122	104	88	0.262	0.310	0.362
	SAW	720	580	470	120	101	86	0.263	0.311	0.362

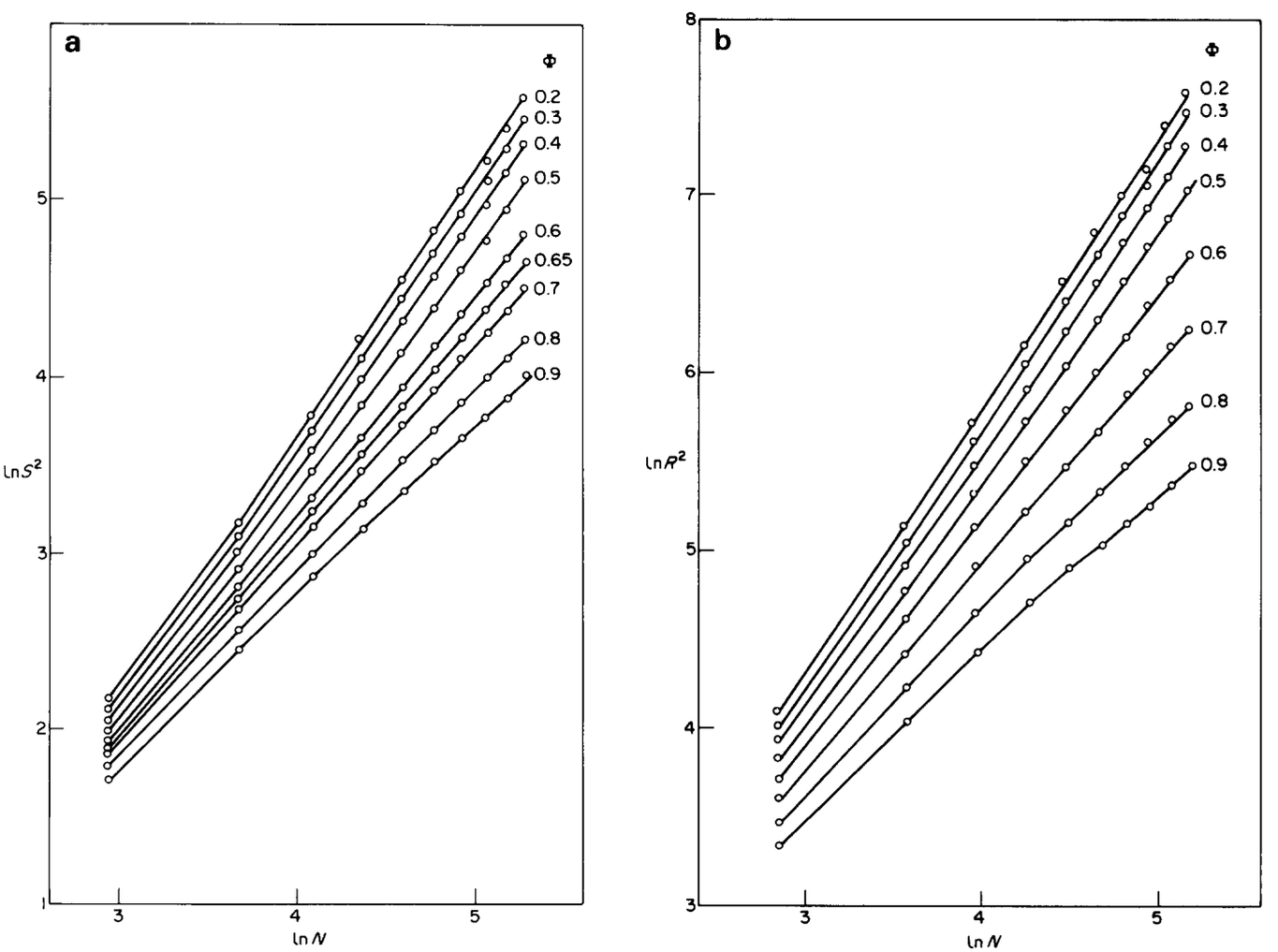

Figure 5 $\ln S^2$ (a) and $\ln R^2$ (b) vs. $\ln N$ for various energies Φ

the variance of γ_s values for 15 sub-ensembles of $M=15000$ chains which were the used larger ensembles (see the formula in the caption of *Table 5*). The errors for γ_s are always less than those for γ_R.

It should be mentioned that, when fitting the lines by the least-square method, we calculated the standard deviation of 'experimental' points from its linear representation for the groups of each five points. For the ensembles of $M=60\times10^3$ IPW's, this value was $5\times10^{-3}-2\times10^{-4}$, being of the same order for S and R and attaining its minimum at $\phi=0.65$. The dependences reproduced on *Figure 5* are practically linear at such energy.

The precise determination of the θ-point is based on the study of the dependences of slopes γ_S and γ_R on N. Taking logarithms of both parts of equation (4), we obtain:

$$\ln S^2=(2\nu_t+\varphi\mu(N^{\phi}\tau))\ln N+\mu(N^{\varphi}\tau)\ln\tau+C$$

where $\mu(x)=\ln f(x)/\ln x$ is a limited function which tends to its limiting values $\pm\mu_{\pm}$ with $x\to\pm\infty$. Assuming that $\mu(x)$ has only a single root $x=0$, i.e. $T=\theta$, one can conclude that, for long chains, $\gamma_s(N)$ chains have to increase above the θ-point, diminish below it and be constant for $T=\theta$.

As it can be seen from *Figures 5* and *6*, the values of γ_x for $\phi<0.65$ increase with the increase of N. This means that the macromolecules become more extended. On the

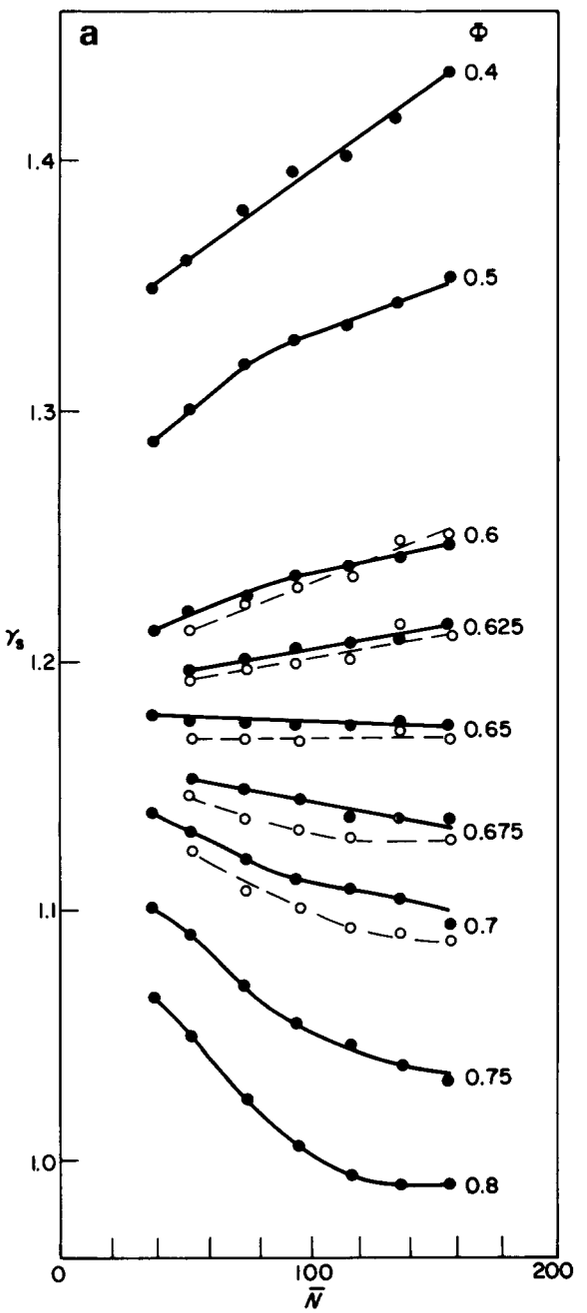

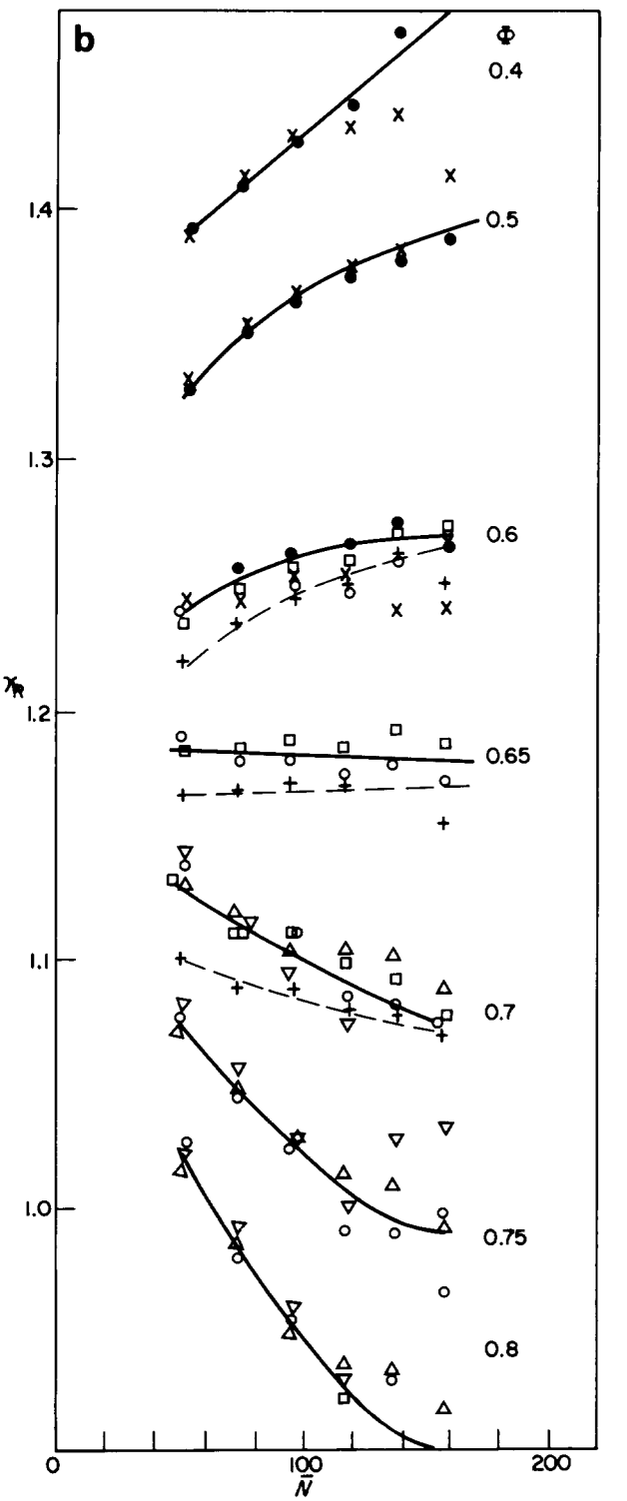

Figure 6 The slopes γ_S (a) and γ_R (b) vs. N for various energies Φ. The linear interpolations have been made according to 5 points. The averaging over different ensembles have not been carried out: (a) (●) IPW; (○) SAW; (b) (×) I; (●) II; (○) III; (□) IV; (△) V; (▽) VI; (+) VII

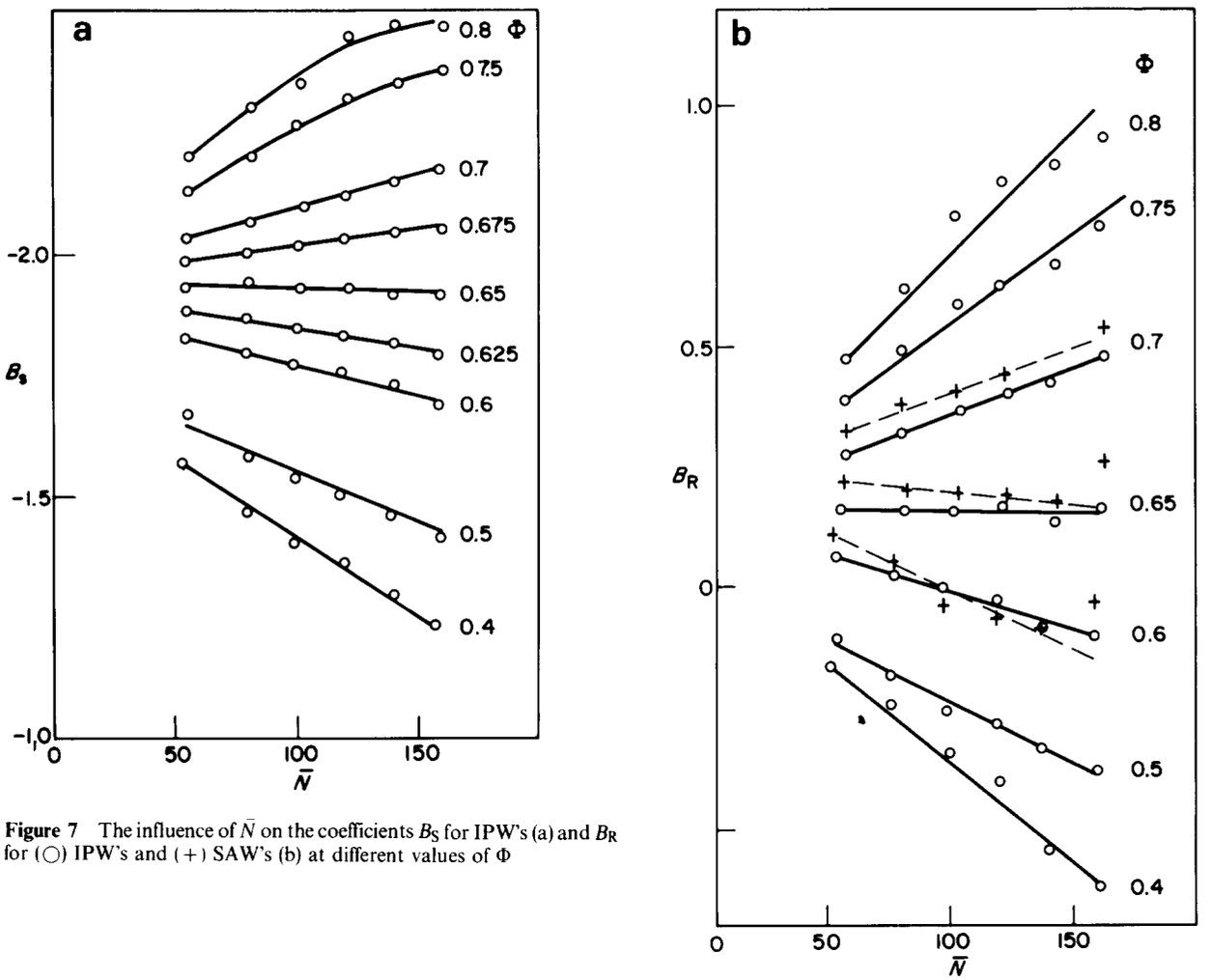

Figure 7 The influence of $\bar{N}$ on the coefficients B_S for IPW's (a) and B_R for (○) IPW's and (+) SAW's (b) at different values of Φ

Table 5 The values of the slope γ_S computed for the groups of 5 points corresponding to the values of N placed in the left column. The errors are given in the brackets, e.g. 0.933 (15) means 0.933 ± 0.015

Values of N	$\bar{N}$	Φ 0.5	0.6	0.625	0.65	0.675	0.7	0.75	0.8
19–(20)–99	51	1.300(2)	1.220(1)	1.198(2)	1.177(2)	1.155(2)	1.132(2)	1.090(3)	1.051(4)
39–(20)–119	73	1.321(4)	1.227(2)	1.201(2)	1.174(2)	1.149(2)	1.121(2)	1.070(5)	1.024(8)
59–(20)–139	95	1.331(4)	1.235(4)	1.206(5)	1.175(3)	1.145(4)	1.113(5)	1.056(7)	1.007(10)
79–(20)–159	116	1.336(6)	1.237(6)	1.208(6)	1.173(5)	1.139(5)	1.110(7)	1.045(10)	0.993(15)
99–(20)–179	137	1.344(8)	1.243(8)	1.210(6)	1.177(5)	1.138(6)	1.104(9)	1.038(15)	0.990(20)
119–(20)–199	157	1.354(10)	1.248(10)	1.216(10)	1.175(6)	1.137(10)	1.095(10)	1.032(20)	0.990(30)

other hand, when $\Phi > 0.65$, the values of γ_x decrease with the growth of N, tending to the value $\gamma_x = 1$ for globular structures (for $\Phi \geqslant 0.8$, the value of γ_R appears to be less than 1, but for longer chains, with $N \to \infty$, it must approach unity from below).

When $\Phi = 0.65$, the values of γ_S and γ_R preserve the same value inside the whole region of observed N values. This allows us to adopt the value of $\Phi = \Phi_\theta = 0.65$ ($\theta = 1/\Phi_\theta = 1.54$) as the θ-point, and the value of $\gamma_x = 2\nu_t = 1.175$ as the corresponding tricritical exponent.

The detailed data concerning the values of quantity Φ_θ and tricritical exponent $\gamma_x = 2\nu_t$ are given in *Table 6*, in which a comparison is also made between the values, obtained for molecular mass dependences of S^2 and R^2 for IPW- and SAW-ensembles. A good agreement of these values is demonstrated.

In summary, we can assert that with a high degree of reliability that $\Phi_\theta = 0.65 \pm 0.05$, i.e. $\theta = 1/\Phi = 1.55 \pm 0.15$, and $2\nu_t = 1.17 \pm 0.07$.

The other characteristics of a chain will now be discussed, which allow an estimate of the value of Φ_θ. The thermodynamical characteristics of the system are represented in *Figures 8* and *9*. The dependences of the reduced mean energy (the number of contacts) per monomer U/Φ *versus* $1/\Phi$ and N are rather smooth both for IPW's and for SAW's (see *Table 3* and *Figure 8*). Unfortunately, we have not been able to investigate in the region of higher values of Φ, where the relative energy U/Φ becomes independent of the temperature $1/\Phi$.

The temperature dependence of C, the specific heat, shown in *Figure 9* for the chains of 199 and 100 segments seems to have a faintly marked maximum, biased from the above-determined value of θ towards the region of lower temperatures. However, the error of determination of the specific heat is very high at large Φ values, and reaches 50%. Therefore, the results obtained do not contradict the previous one. It should be noted that at large values of Φ the effective number of chains in the ensemble falls to the

Table 6 Results of determination of ϕ_θ and $2\nu_t$ according to the slopes of curves $\ln S^2(\ln N)$ and $\ln R^2(\ln N)$ for IPW's and SAW's

	ϕ_θ		$2\nu_t$	
	S^2	R^2	S^2	R^2
IPW's	0.65±0.01	0.64±0.02	1.175±0.005	1.20±0.02
SAW's	0.65±0.01	0.65±0.02	1.170±0.005	1.165±0.02

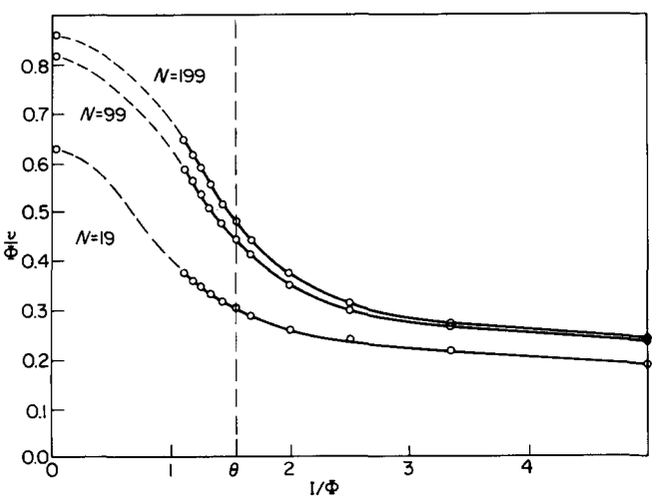

Figure 8 The reduced mean energy per monomer U/Φ vs. $1/\Phi$ for various chain lengths N. (The data for IPW's and SAW's coincide). The ratio of number of contacts to N in the limit of $1/\Phi \to 0$ plotted by the dashed lines

value of $M_{eff} \sim 10$, even if the total number of chains in the ensemble $M = 140\,000$. That is why some unique mostly tightly coiled conformations (of a spiral type, perhaps), may cause tremendous jumps of the average specific heat. Unfortunately, we are still not able to explain the effect of the non-monotonic dependence of C vs. N (see *Figure 9b*), which takes place at different values of Φ including those in the vicinity of Φ_θ, where the spread of C is not large, due to M_{eff} being rather high. As can be seen from *Figure 9b*, the deviations of $C(N)$ from smooth curve have different signs for IPW's and SAW's.

Figure 10 shows the dependence of the ratio of R^2/S^2 vs. N for various values of Φ, near to Φ_θ. This ratio appears to be sensitive to the type of ensemble chosen (IPW or SAW). This can be explained by the fact that the probability of the chain end to enter into the coil is less for IPW than for SAW. The ratio R^2/S^2 characterizes the form of the coil, so the value of $\Phi = \Phi_1$, at which this ratio has the random-coil value $R^2/S^2 = 6$, is of some interest. It can be seen from *Figure 10* that the ratio diminishes with the increase of Φ (at any fixed N). Value Φ_1 is equal to 0.625±0.025 and 0.60±0.025 for IPW and SAW-ensembles, respectively.

The other characteristic value of Φ is value Φ_2, corresponding to the change of the sign of molecular-mass dependence of the ratio R^2/S^2, increasing with N for $\Phi < \Phi_2$ and decreasing with N for $\Phi > \Phi_2$. Φ_2 is equal to 0.7±0.025 for IPW's and 0.65±0.25 for SAW's. The closeness of Φ_1 and Φ_2 to Φ_θ confirms the correctness of the procedures of the θ-point determination.

DETERMINATION OF THE CROSS-OVER EXPONENT φ

In order to determine φ we use the scaling expression equation (4), according to which:

$$S^2/N^{2\nu_t} \sim f(N^\varphi \tau)$$

Hence, if one selects from the available data the points, for which the quantity $S^2/N^{2\nu_t}$ is constant, the value of $N^\varphi\tau$ must also be constant at these points. In other words, one can expect the level curves (lines of fixed values) of function $F = -\ln S^2 + 2\nu_t \ln N$ to be the straight lines on the $\ln\tau - \ln N$ plane, these lines being determined by the relationship:

$$\ln\tau = K - \varphi \ln N \qquad (8)$$

where K is expressed by the corresponding value of function F. Let us dwell on the definition of the reduced temperature τ. The temperature in the computer experiment is simulated by the quantity $1/\Phi = -kT/\varepsilon$, which

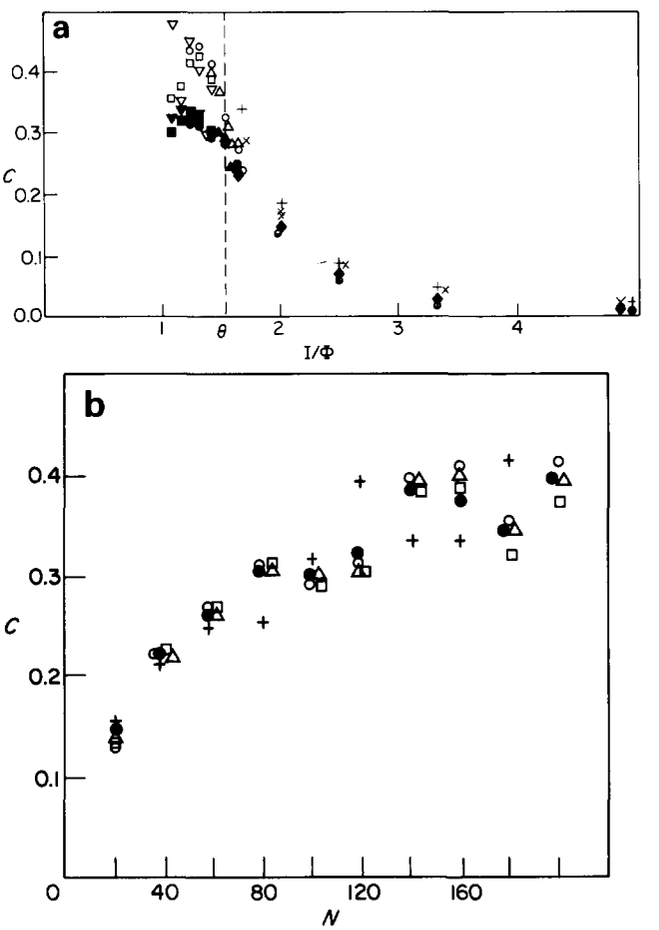

Figure 9 The specific heat C vs. $1/\Phi$ in various ensembles of IPW's (a).

$N=99$	$N=199$	
◆	+	I
◑	×	II
●	○	III
▲	△	IV
■	□	V
▼	▽	VI

Specific heat vs. chain length length N at $\Phi = 0.7$ for various ensembles of IPW's and SAW's (b). The Roman numerals are the numbers of ensembles in *Table 1*. (○) III; (△) IV; (●) V; (□) VI; (+) VII

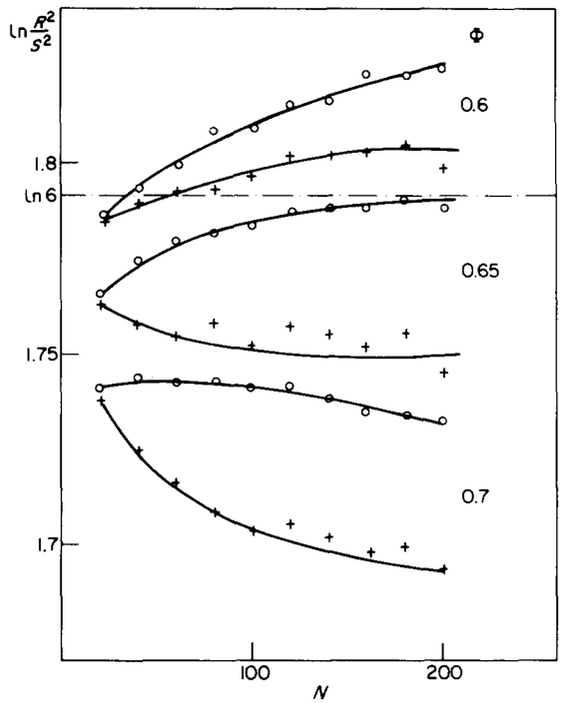

Figure 10 $\ln(R^2/S^2)$ vs. N for various values of Φ in the ensembles of IPW's (IV) and SAW's (VII), that have been generated for $\Psi=0.3$. (+—+) VII; (○——○) IV

varies in the broad interval. (The case of $\Phi=0$ corresponds to $T\rightarrow\infty$). On the other hand, it is always assumed in scaling relations like equation (4) that τ is a small value, undoubtedly, $\tau<1$. In order to satisfy this condition, it is reasonable to define τ as:

$$\tau=\begin{cases}\dfrac{T-\theta}{T}=1-\dfrac{\Phi}{\Phi_\theta}, & \Phi<\Phi_\theta\\[2ex] \dfrac{\theta-T}{\theta}=1-\dfrac{\Phi_\theta}{\Phi}, & \Phi>\Phi_\theta\end{cases}$$

The level-curves of function $F_1=[2\nu_t\ln N-\ln S^2-1.58]\times10^3$, plotted on the $\ln N-\ln\tau$ coordinate plane for $2\nu_t=1.176$, $\Phi_\theta=0.65$ are shown in *Figure 11*. The series of points, corresponding to the values of $\Phi=0.5$, 0.6, 0.625 (open circles) and $\Phi=0.675$, 0.70, 0.75 (closed circles) for all chain lengths from 19 to 199, are plotted, and the corresponding values of function F_1 are marked near the points. The value 1.580 is subtracted in order to change the sign of the value of F_1, when crossing the θ-point.

The straight lines, which are the level curves of F_1, are constructed of points determined by interpolation.

The slopes of lines are (from above to below) -0.59, -0.65, -0.61, -0.70 ($\Phi<\Phi_\theta$ broken lines) and -0.60, -0.56, -0.63, -0.66 ($\Phi>\Phi_\theta$, solid lines). These values must tend to the crossover exponent $-\varphi$ when $N\rightarrow\infty$ and $\tau\rightarrow0$, that corresponds to the right low corner of *Figure 11*, where the lines with $F=-80$ and 80 with the slopes of -0.61 and -0.56, respectively, are passing.

The analysis shows that the slopes of level-lines depend strongly on the adopted values of ϕ_θ and $2\nu_t$. The slight change of Φ_θ leads to the great change of $\ln\tau$ in the region of small τ (the lower part of the plot) and exerts almost no influence at large values of τ (upper part of the plot). This leads to the change of slopes of the level curves: the increase of Φ_θ by 0.001 only increases the slope of the level curves by 0.02 at $\Phi>\Phi_\theta$ and decreases it by the same value at $\Phi<\Phi_\theta$.

The variations of $2\nu_t$ exhibit themselves in an analogous way. For $\Phi>\Phi_\theta$ the slopes of the level curves increase with increases in $2\nu_t$; but for $\Phi_\theta>\Phi$ the opposite occurs. Therefore, if $2\nu_t$ increases by 0.001, the slopes of lines with $F_1=40$, and $F_1=80$ increase by 0.02 and 0.006 respectively, and the slopes of lines with $F_1=-40$, and $F_1=-80$ decrease by a similar value. Different signs of the correction on different sides of the θ-point do not allow elimination of the difference in the slopes of lines with $F_1=\pm40$ and $F_1=\pm80$ as plotted in *Figure 11* (the slopes are 0.66–0.70 and 0.56–0.61). The best agreement between the slopes is given by the values of Φ_θ and $2\nu_t$ chosen when constructing the plot of *Figure 11*. As a whole, taking into account some uncertainty in the calculation of φ, one can affirm with sufficient reliability that the value of φ lies between 0.5 and 0.7.

DISCUSSION

The values obtained for $\Phi_\theta=0.65$, $\nu_t=0.588$ and $\varphi=0.6$ allow us to plot all the data of *Figure 2* on the $\ln(N^{2\nu_t}/S^2)-\ln(\tau N^\varphi)$ coordinate plane (*Figure 12*), according to equations (4) and (5). As shown in *Figure 12* all available data lie well on two branches of scaling dependence.

The branch corresponding to $\Phi<\Phi_\theta$ (i.e. the region above the θ-point) approaches the linear asymptote II

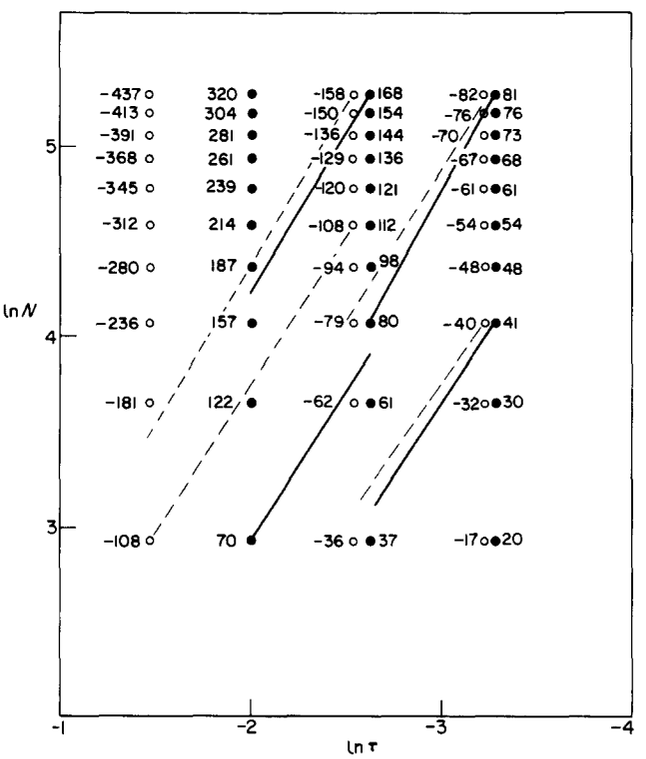

Figure 11 The values of function $F_1=[2\nu_t\ln N-\ln S^2-1.580]\times10^3$, plotted on the plane ($\ln N$, $\ln\tau$). The values of $2\nu_t$ and Φ_θ are $2\nu_t=1.176$, $\Phi_\theta=0.65$. The horizontal series of points, plotted for the values of N from $N=19$ to $N=199$ with the step 20, correspond (from above to below) to the following values of $\phi=0.5$, 0.6, 0.625 (○) and $\Phi=0.75$, 0.7, 0.675 (●). The straight lines connect the points with the equal values of F_1. (If there were not enough points, we made linear interpolation). For $\Phi<\Phi_\theta$ these lines (– – –) correspond to the values of $F_1=-158$, -108, -80, -40 and have the slopes $-\varphi=-0.59$, -0.65, -0.61, -0.70 (from above to below). For $\Phi>\phi_\theta$ (———) $F_1=168$, 80, 70, 40, $-\varphi=-0.60$, -0.56, 0.63, -0.66. This legend and the discussion in the text correspond to the plot, turned 90° clockwise

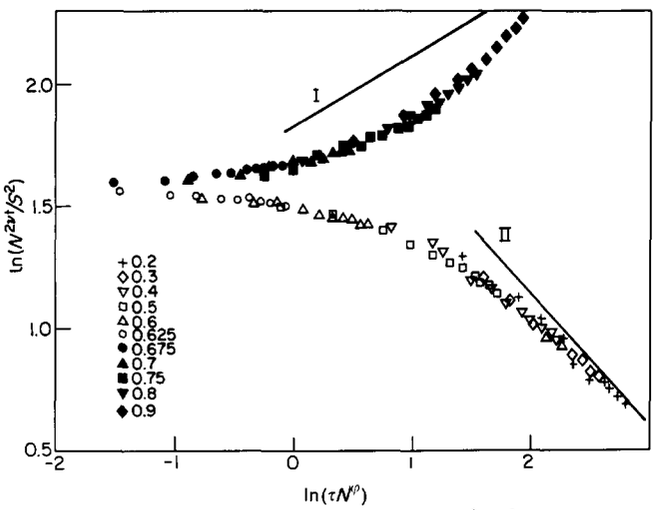

Figure 12 The summarizing scaling plot of $\ln(N^{2\nu_t}/S^2)$ vs. $\ln(\tau N^{\varphi})$ above the θ-point (lower branch) and below the θ-point (upper branch). The values of $2\nu_t$, ϕ_θ, φ are taken as follows $2\nu_t = 1.176$, $\phi_\theta = 0.65$, $\varphi = 0.6$. The slopes of line I and II are $\mu_- = 0.29$ and $-\mu_+ = -0.54$ respectively. Line I crosses the ordinate axis at $\ln(2\pi) \approx 1.84$. Points correspond to different Φ (as indicated)

with the slope $-\mu_+ = -0.54$, where the value of μ_+ is determined by equation (6) for the value of ν_t found in the above. When $\Phi > \Phi_\theta$ (below the θ-point) equation (6) yields $\mu_- = 0.29$, which specifies the slope of the asymptotic line I in *Figure 12*.

The position of this line can easily be determined by the following simple procedure. At very large attractive energies Φ when $\tau \approx 1$ all the chains must assume the most dense conformation with the gyration radius $S^2 = N/2\pi$. Hence, the equation of line I in *Figure 12* can be written as $y = \mu_- x + \ln 2\pi \approx 0.29x + 1.84$. As it is seen from *Figure 12* all the points of the branch $\Phi > \Phi_\theta$ lie under line I. (The sizes of the chains below the θ-point are larger than follow from the scaling relations). In the interval of values of $\Phi = 0.8 - 0.9$, the slope of the branch is steeper than slope μ_- of line I. The corresponding values of γ_S and γ_r plotted in *Figure 6* are less than 1 for these energies. As a whole, the deviation of the branch slope from the asymptotical one is not large.

Thus, our data contradict the conclusions of early theoretical works, based on the renormalization group approach[1,4], according to which the chains near the θ-point ($d = 2$) are random, i.e., the exponent $2\nu_t$ is near to unity and, respectively, the exponent μ_- is near to zero. The value obtained for $2\nu_t$ appears to be intermediate between the values of Refs 1 and 4, and the values yielded by the approach of the meanfield theory. At the same time, the cross-over exponent φ is close to one computed in the works[1,4].

After our work was finished, Kholodenko and Freed[11] have shown that the modification of the renormalization-group approach yielded the new values of the exponents ν_t and φ. It appears that the value of ν_t obtained in our paper, is close to these results, and the value of φ is also similar.

As mentioned in the introduction, the calculations of conformations of the model lattice chains have been carried out previously, the most detailed being the work of Baumgärtner[14]. The comparison shows the proximity of our results and the numerical data of the work[14], whereas the conclusions of both works are opposing. Baumgärtner proceeds from the validity of the theoretical values of critical exponents[1,4], analysing the numerical experiment on their grounds. We consider that our method of analysing the computer experiment is more reliable.

It should be mentioned that our results agree with the experimental data of Ref. 25, in which the value of $\nu_t = 0.56$ have been obtained for poly(methyl methacrylate), adsorbed on the water surface at $t = 16.5°C$, that is close to θ-conditions.

Notes added in proof

(1) Recently a new self-avoiding walk named indefinitely growing (IGSAW) has been introduced. (Kremer, K. and Lyklema, J. W. *J. Phys. A:Math. Gen.* 1985, **18**, 1515–1531.) The method of constructing IGSAW is the same as that for IPW. The only difference is that the partition function of IGSAW is calculated without the Rosenbluth's weight w. (Truly kinetic model).

(2) The careful analysis shows that the effect of non-monotonic dependence of C vs. N (see *Figure 9b*) is an artifact of the computer rounding errors and can be removed by a slight modification of the routine.

REFERENCES

1 De Gennes, P. G. *J. Phys. Lett.* 1975, **36**, L-55
2 Stephen, M. J. and McGauley, J. L. *Phys. Lett.* 1973, **44A**, 89
3 De Gennes, P. G. 'Scaling concepts in Polymer Physics', Cornell Univ. Press, Ithaca and London, 1979
4 Stephen, M. J. *Phys. Lett.* 1975, **53A**, 363
5 Riedel, E. K. and Wegner, F. *Phys. Rev. Lett.* 1972, **29**, 349
6 Derrida, B. *J. Phys.* 1981, **A14**, L-5
7 Gassberger, P. *Z. Phys.* 1982, **B48**, 255
8 Nienhuis, B. *Phys. Rev. Lett.* 1982, **49**, 1062
9 Watts, M. G. *J. Phys.* 1974, **A7**, 489
10 Khokhlov, A. R. *Polymer* 1981, **22**, 447
11 Kholodenko, A. L. and Freed, K. F. *J. Phys.* 1984, **A17**, L-191
12 Birshtein, T. M. and Zhulina, E. B. in 'Matemat. Metody Issled. Polymerov', Poustchino, 1983, p. 3
13 Flory, P. J. 'Principles of Polymer Chemistry', Cornell Univ. Press, Ithaca, NY, 1971
14 Baumgärtner, A. J. *J. Phys.* 1982, **43**, 1407
15 Tobochnik, J., Webman, I., Lebowith, J. L. and Kalos, M. H. *Macromol.* 1982, **15**, 549
16 Meirovitch, H. *J. Chem. Phys.* 1983, **79**, 502
17 Rosenbluth, A. W. and Rosenbluth, M. N. *J. Chem. Phys.* 1955, **23**, 356
18 McCrackin, F. L., Masur, J. and Guttman, C. L. *Macromol.* 1973, **6**, 859
19 Elyashevitch, A. M. and Skvortsov, A. M. *Molec. Biol.* 1971, **5**, 204
20 Birshtein, T. M., Sariban, A. A. and Skvortsov, A. M. *Vysokomol. Soedin.* 1975, **17A**, 1962
21 Birshtein, T. M., Elyashevitch, A. M. and Morgenshtern, L. A. *Biophys. Chem.* 1974, **1**, 242
22 Lifshitz, I. M., Grosberg, A. Yu. and Khokhlov, A. R. *Uspekhi Phys. Nauk.* 1979, **127**, 353; *Rev. Mod. Phys.* 1978, **50**, 683
23 Birshtein, T. M. and Ptitsyn, O. B. 'Conformations of Macromolecules', Interscience, New York, 1966
24 Flory, P. 'Statistical mechanics of chain molecules', Interscience, New York and London, 1969
25 Vilanove, R. and Rondelez, F. *Phys. Rev. Lett.* 1980, **45**, 1502